Paper

Compensation of the Non-Sinusoidal Electromotive Force with Multiple-Frequency Resonant Controller for a PMLSM

Remy Ghislain* Non-member
Degobert Philippe* Non-member
Barre Pierre-Jean* Non-member
Hautier Jean-Paul* Non-member
Zeng Jia* Non-member

This paper presents how to compensate for the non-sinusoidal electromotive force (EMF) of the permanent magnet linear synchronous motor (PMLSM) with a multiple-frequency resonant controller. After the modeling of the non-sinusoidal EMF in a PMLSM, the multiple-frequency resonant controller is proposed to control the PMLSM in order to compensate for the negative influence of such EMF. After explaining the discrete resonant controller theory, the effectiveness of the suggested method is verified on a test bench equipped with a Rexroth LSP120C linear motor and a dSPACE DS1005 real-time controller board.

Keywords: PMLSM, non-sinusoidal electromotive force, discrete resonant controller, thrust control

1. Introduction

Nowadays, with its attractive characteristics, the Permanent Magnet Linear Synchronous Motor (PMLSM) is widely used in high speed and high precision drive systems [1]. Generally, the field-oriented control with PI controllers in the $(d-q)$ synchronous reference frame is used to control such systems [2]. Yet this method is not capable of compensating for the negative influence of non-sinusoidal EMF, which will bring on undesired thrust ripples [3].

For a PMLSM with non-sinusoidal back-EMF, the excitation currents should comprise appropriate harmonics in order to suppress the thrust ripple components [4][5]. Direct Torque Control (DTC) and the Multiple Reference Frame (MRF) theory have been applied to resolve this problem [6][7]. However, each method has its troublesome drawbacks: large torque ripple at low speeds, variable switching frequency [8] for DTC; complex control structure and large computation time requirement for the MRF [9]. Secondly, the switching frequency varies according to the motor speed as well as to the hysteresis bands of thrust and flux [10]. Although some methods have been proposed to fix this frequency, too many switchings are not necessary and they don't contribute to reducing the control errors [11]. Finally, although various techniques of thrust estimation and flux observation have been proposed to generate the necessary feedback signals, the difficulties in accurate estimation of instantaneous thrust make it impossible to fully cast off the negative influence from motor parameter variations [12].

In this paper, we will propose to use the multiple-frequency resonant controller to compensate for the influence of the non-sinusoidal EMF. By associating an arbitrary number of resonant elements with each other, this type of controller can eliminate the steady-state control errors of the fundamental component as well as the harmonics components at the same resonant frequencies [13].

After the modeling of the PMLSM with non-sinusoidal back EMF, optimal current waveforms are suggested to reduce the thrust ripple caused by the harmonics of the back-EMF. By using multi-frequency resonant controllers, the load currents in the PMLSM can follow the reference currents perfectly, and thereby, significantly reduce the thrust ripple of the PMLSM.

2. Influence of Non-sinusoidal EMF on Thrust

In this section, the model of a permanent magnet linear synchronous motor is presented. We make the following assumptions:

- Three-phase motors are without saturation and cogging effects, Y-connected, with inaccessible neutral wire;
- Non-sinusoidal back electromotive force are considered;
- The waveforms of EMF and the magnetostatic flux of

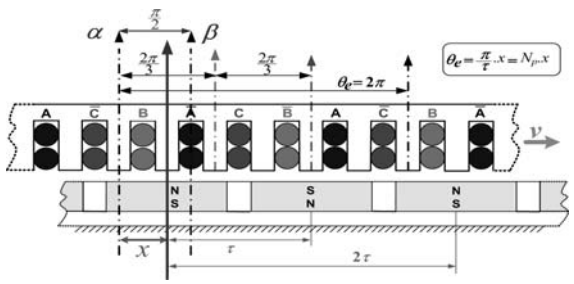

Fig. 1. Principle schematic of PMLSM

* Motion Control of High Dynamic Machine-Tools
Technological Research Team CEMODYNE, ERT Int 1022
Laboratory of Power Electronics and Electrical Engineering of Lille
L2EP, ENSAM Lille, 8, Bd Louis XIV, 59046 Lille, France

magnets are half-wave symmetrical (no even harmonics);
- The resistances and inductances in three phases are constant and identical.

Fig. 1 depicts the simplified schematic of a short primary PMLSM. To adapt the proposed control structure, this model is established in the Concordia reference frame, called the (α-β) diphase stationary reference frame [14].

When the back-EMF wavefoms are half-wave symmetrical, they have no even harmonics and can be expressed by:

$$[e_0(t)] = -v \cdot \hat{\phi}_f \cdot \sum_{n=1}^{\infty} \lambda_{2n-1} \begin{bmatrix} \sin[(2n-1)N_p x] \\ \sin[(2n-1)(N_p x - 2\pi/3)] \\ \sin[(2n-1)(N_p x - 4\pi/3)] \end{bmatrix} \quad \cdots\cdots (1)$$

Wherein $\hat{\phi}_f$ denotes the maximum value of magnetic excitation flux per phase in the (abc) stationary reference frame. The coefficients λ_{2n-1} represent the relative magnitudes of the $(2n-1)^{\text{th}}$ back-EMF harmonic. $N_p = \pi/\tau_p$ is the electrical position constant of the PMLSM (τ_p: step between two consecutive magnetic poles of the secondary) [15]. Finally, v denotes the linear speed of the mobile part.

Then, the voltage equations of the PMLSM in the Concordia reference frame can be expressed as:

$$[V_{\alpha\beta}] = \left([R] + \frac{d[L_{\alpha\beta}]}{dt}\right) \cdot [I_{\alpha\beta}] + [L_{\alpha\beta}] \cdot \frac{d[I_{\alpha\beta}]}{dt} + \sqrt{\frac{3}{2}} N_p v \hat{\phi}_f \cdot \sum_{n=1}^{\infty} \lambda_{2n-1} \begin{bmatrix} K_\alpha^{2n-1} \cdot \sin[(2n-1)\theta] \\ K_\beta^{2n-1} \cdot \cos[(2n-1)\theta] \end{bmatrix} \quad \cdots\cdots (2)$$

R represents the stator resistances; $V_{\alpha\beta}$ and $I_{\alpha\beta}$ denote the voltage and current vectors, respectively. The coefficients K_α^{2n-1} and K_β^{2n-1} are triply periodic functions.

$$\begin{cases} K_\alpha^{2n-1} = -\dfrac{2}{3}\left[1 + \cos\left(\dfrac{2n-1}{3} \cdot \pi\right)\right] \\ K_\beta^{2n-1} = \dfrac{2}{\sqrt{3}} \sin\left(\dfrac{2n-1}{3} \cdot \pi\right) \end{cases} \quad \cdots\cdots (3)$$

Table 1 gives their values based on the independent periods n:

The inductance matrix is given by:

Table 1. Value of two periodic functions

Independent periods n	K_α^{2n-1}	K_β^{2n-1}
1	-1	1
2	0	0
3	-1	-1
4	-1	1
…	…	…

Table 2. Coefficients of Electromotive Force harmonics

Coefficients names	λ_1	λ_5	λ_7	λ_{11}
Coefficients values	1	-0.0267	0.000423	0.000459

$$[L_{\alpha\beta}] = \begin{bmatrix} L_s - M_s & 0 \\ 0 & L_s - M_s \end{bmatrix} \quad \cdots\cdots (4)$$

The electromagnetic thrust generated by the PMLSM can be derived by using co-energy techniques [16], which are created by the mutual coupling between the winding currents and the permanent magnetic field. The thrust T_e may be expressed as:

$$T_e = \sqrt{\frac{3}{2}} \cdot N_p \hat{\phi}_f \cdot \begin{bmatrix} i_\alpha & i_\beta \end{bmatrix} \cdot \begin{bmatrix} -\sum_{n=0}^{\infty} \lambda_{6n+1} \sin[(6n+1)\theta] - \sum_{n=1}^{\infty} \lambda_{6n-1} \sin[(6n-1)\theta] \\ \sum_{n=0}^{\infty} \lambda_{6n+1} \cos[(6n+1)\theta] - \sum_{n=1}^{\infty} \lambda_{6n-1} \cos[(6n-1)\theta] \end{bmatrix} \quad \cdots\cdots (5)$$

If we neglect the effects of EMF harmonics, the waveforms of currents i_α and i_β should be sinusoidal. By substituting these coefficients into (5), we can notice that thrust ripples will be introduced by a non-sinusoidal EMF.

The studied PMLSM is a Rexroth LSP120C linear motor. The coefficients of EMF harmonics are experimentally identified [17] and are listed in Table 2:

We can notice in Table 2 that the thrust ripple caused by the 5^{th} emf harmonic could reach 2.67%, which is the dominant ripple source. However, those caused by the 7^{th} and 11^{th} harmonics are so slight (0.1% in total) that their influence can be neglected.

3. Thrust Control Scheme

3.1 Design of the Control Structure In this section, we establish the PMLSM digital thrust control scheme in the Concordia reference frame, as in Fig. 2:

Wherein T_e^* represents the reference thrust. The reference excitation currents (i_α^* and i_β^*) are generated according to the mover position x and to the reference thrust T_e^*, which are given by (6) and implemented in the "Excitation Currents Generator" block.

$$\begin{cases} i_\alpha^* = \dfrac{T_e^* \cdot [-\sin(\theta) + \lambda_5 \cdot \sin(5\theta)]}{\sqrt{\frac{3}{2}} \cdot N_p \cdot \hat{\phi}_f \cdot \left(1 - \lambda_5^2\right)} \\ i_\beta^* = \dfrac{T_e^* \cdot [\cos(\theta) + \lambda_5 \cdot \cos(5\theta)]}{\sqrt{\frac{3}{2}} \cdot N_p \cdot \hat{\phi}_f \cdot \left(1 - \lambda_5^2\right)} \end{cases} \quad \cdots\cdots (6)$$

The three-phase load currents are measured, tranformed and regulated by two multiple-frequency resonant controllers

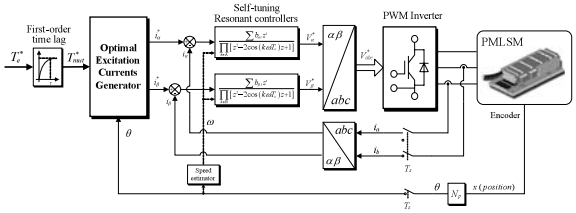

Fig. 2. PMLSM digital thrust control scheme using multiple-frequency resonant controllers

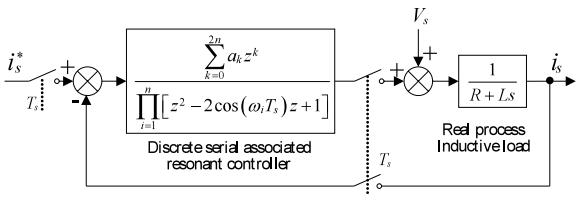

Fig. 3. Discrete model of an AC current control system using a multiple-frequency resonant controller

in the Concordia reference frame. The mover position is detected and fed into the "Excitation Currents Generator" block to generate instantaneous reference thrust. The angular speed ω is estimated and fed into the multiple-frequency resonant controllers so that they can adapt to the reference currents with time-varying frequency.

3.2 Discrete Resonant Controller Theory The general transfer function of a discrete multiple-frequency resonant controller is given by [13]:

$$F(z) = \frac{\sum_{k=0}^{2n} a_k z^k}{\prod_{i=1}^{n}\left[z^2 - 2\cos(\omega_i T_s)z + 1\right]} \quad \cdots\cdots\cdots\cdots (7)$$

$$\{i, n \in \mathbf{N}; k \in \mathbf{Z}; a_k, \omega_i \in \mathbf{R}\}$$

Wherein k denotes the number of associated resonant elements and ω_i corresponds to each concerned resonant frequency. T_s is the system sample time.

Fig. 3 depicts the discrete model of an AC current control system, in which the inductive load is controlled by a multiple-frequency resonant controller.

3.3 Resonant Controller Tuning Principle In many cases, the control system is required to track current command with time-varying frequency. For example, in the adjustable speed motor control applications, the frequency of phase currents varies with the rotor speed. To resolve this problem, the resonant controller is reconfigured by adjusting its coefficients according to the input frequency during its operation. This type of controller is called a self-tuning resonant controller [18].

Our technique for the self-tuning controller design requires to:

- Choose the number of frequencies to compensate.
- Identify the closed-loop characteristic polynomial using the control system described in Fig. 3:
- Define a pole placement technique and a stability margin.
- Calculate the coefficients of the resonant controllers in order to adapt the closed-loop characteristic polynomial to a criterion polynomial, which describes the desired closed-loop poles.
- Verifiy the system stability in the Bode diagrams of the open-loop and closed-loop systems.

Some researchers have suggested implicit pole assignment algorithms for the self-tuning controller design, in which the controller coefficients are estimated directly without the need for polynomial identification [19]. However, if the closed-loop poles are not properly selected, the computational savings using implicit algorithms are often offset by slow convergence

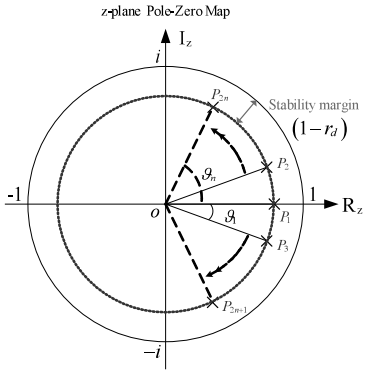

Fig. 4. Pole locations of the closed-loop system designed by Generalized Stability Margin

phase systems.

Whenever the system varies, the changed characteristic polynomial should be renewably identified by this criterion polynomial so as to adjust the controller coefficients.

The closed-loop characteristic polynomial is obtained using the impulsed response transform [18]:

$$P(z) = R\left(z - e^{-T_s \cdot R/L}\right)\prod_{i=1}^{n}\left[z^2 - 2\cos(\omega_i T_s)z + 1\right] + \left(1 - e^{-T_s \cdot R/L}\right)\sum_{k=0}^{2n} a_k z^k \quad \cdots\cdots\cdots\cdots (8)$$

Nowadays, it is well-known that the performance specifications of a control system (*e.g.* settling times, overshoot and damping) depend on the pole locations [19]. Root locus, Bode and Nyquist diagrams are classical methods using a graphical representation of the effects of controller gains on system response [20].

Another technique is to determine the controller coefficients by assigning the same stability margin to all closed-loop system poles. To achieve robust pole assignment for the time-variant control systems, the design criteria should be appropriately selected so that the closed-loop poles are constrained within desired regions, regardless of the variations in system parameters and/or in dimension [14]. For a control system using n-frequency resonant controllers, the criterion defined by this method is expressed by:

$$P_{ref}(z) = \lambda(z - r_d)\prod_{i=1}^{n}\left[z^2 - 2r_d\cos(\theta_i)z + r_d^2\right] \cdots\cdots (9)$$

$$\{\lambda, r, r_d, \theta_i \in \mathbf{R}; i, n \in \mathbf{N}\}$$

All closed-loop poles identified by this polynomial will be settled on a circle in the z-plane Pole-Zero Map [21], as in Fig. 4.

The principle of self-tuning pole assignment design then consists in solving equation (8) with the *a priori* knowledge of polynomial P_{ref} (s) to obtain the controller coefficients a_k. In our case, they will be expressed as a function of the current frequencies ω_i.

$$P(z) = P_{ref}(z) \cdots\cdots\cdots\cdots (10)$$

The solution is unique if the following condition is fulfilled:

$$\text{order}(P_{ref}) = m, \quad \text{with} \quad m \leq 2n + 1 \cdots\cdots\cdots\cdots\cdots (11)$$

The complexity of this solution depends on the order m of the criterion polynomial. In general, m is chosen as equal to $2n + 1$ so that all closed-loop poles are completely controllable, which gives a lot of freedom in the controller design. The fundamental methodological problem then lies in determining the locations of closed-loop poles through this polynomial in order to deal with the trade-off between performances and robustness. The radius of this circle is defined by r_d, which determines the stability margin as well as the dynamic response of the control system. A similar technique can be used for the continuous model: The closed-loop poles are placed on a vertical line with a stability margin defined by r in the s-plane Pole-Zero Map [22] with $r_d = e^{-\mathrm{rTs}}$.

Here, the stability margin is fixed using $r_d = 0.9$, in order to maintain the system stability for a range of ω_i from 0 to 1000 rad/s [18]. The angles θ_i are generally assigned by the resonant frequencies as $\theta_i = \omega_i T_s$. In variable frequency applications, the tuning of θ_i according to the current frequency ω_i in real time requires too much computation. However, if appropriate values are assigned to θ_i, satisfying performances can be achieved for a wide range of current frequencies. The maximum values of current frequencies are designed according to $\theta_i = \max(\omega_i)T_s$.

3.4 Resonant Controller Application The number and frequencies of associated resonant elements depend on the references and/or the characteristics of each decoupled subsystem.

In this way, the tracking of the reference currents and the rejection of disturbances from non-sinusoidal back-EMF can be simultaneously realised.

In our case, the two controllers have identical structures with two resonant frequencies—the fundamental and the 5th harmonic. Fig. 5 illustrates the Bode diagrams of the open-loop transfer function of the control system using a two-frequency resonant controller. We can note that infinite gains are produced at the concerned frequencies (ω_0, $5\omega_0$), regardless of the variation in ω_0. This ensures that the steady-state error at these frequencies can be completely eliminated.

In the meantime, they have almost identical crossover frequency and high-frequency characteristics, which guarantees that the control system possesses the same dynamic response for any current frequency.

The Bode diagram of the closed-loop transfer function (Fig. 6) presents a characteristic of unity gains (0 dB) and zero phases at the selected frequencies, further confirming that the control system can perform zero steady-state error at these frequencies.

4. Experimental Results

The proposed approach is experimentally verified on a laboratory test system equipped with a Rexroth LSP120C linear motor (Fig. 7).

The control scheme depicted in Fig. 2 is implemented in a dSPACE DS1005 real-time digital control card to drive the PMLSM through an IGBT inverter. We have used a Heindenhain exposed linear encoder with a grating period of 20 μm, which is a high precision incremental encoder, to detect the mover position.

Table 3 lists the specifications of the test bench parameters:

Fig. 8 and Fig. 9 present the experimental references, measurements and estimations of currents and thrust. Fig. 8 shows the results from an AC current control system using one-frequency resonant controllers. Fig. 9 shows the results from an AC current control system using two-frequency resonant controllers. In both cases, the load currents are very close to their references. The maximal delay of the load currents stays under 0.5 ms, even if brutal changes occur in current references. When the non-sinsuoidal emf is not compensated (Fig. 8), we notice a ripple of 5% on thrust estimation. After the compensation using two-frequency resonant controllers, the ripple is reduced to 1% of the estimated thrust. Nevertheless, the load current in the second case is noisier (by over 300%), because we need to inject the measure of the 5th harmonic of the currents.

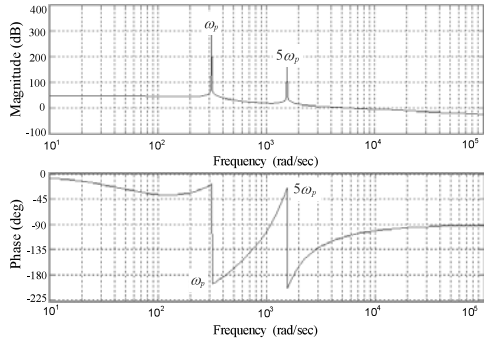

Fig. 5. Verification in the open-loop Bode diagram

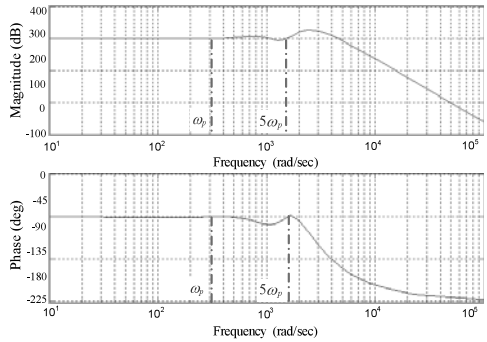

Fig. 6. Verification in the closed-loop Bode diagram

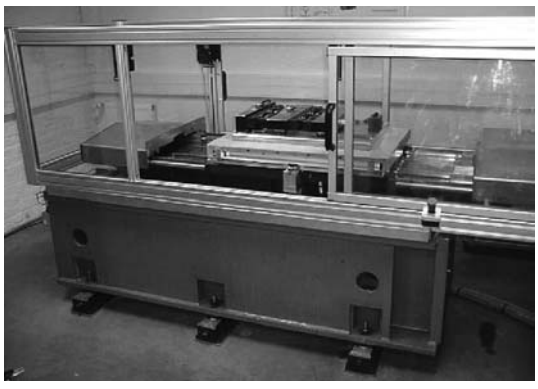

Fig. 7. Linear Motor Rexroth LSP120C

Table 3. Specifications of test bench parameters

Parameter names	Parameter values
Rated current; Maximum current	51 [A]; 175 [A]
Rated voltage	220 [V]
Rated thrust; Maximum thrust	3100 [N]; 7800 [N]
Attraction force	20100 [N]
Pole pitch	τ_p = 37.5 [mm]
Electrical position constant:	N_p = 83.8 [rad/m]
Armature resistance:	R = 1.1 [Ω]/ phase
Cyclic inductance:	L_{s0} - M_{s0} = 6.0 [mH]
Harmonic values of back-EMF	λ_5 = -0.00532
	λ_7 = 6.0486 x 10-5
	λ_{11} = 4.1172 x 10-5
Max value of magnet flux per phase	$\hat{\phi}_f$ = 0.65 [Wb]
DC-link voltage	V_{dc} = 580 [V]
IGBT switching frequency	f_c = 10 [kHz]

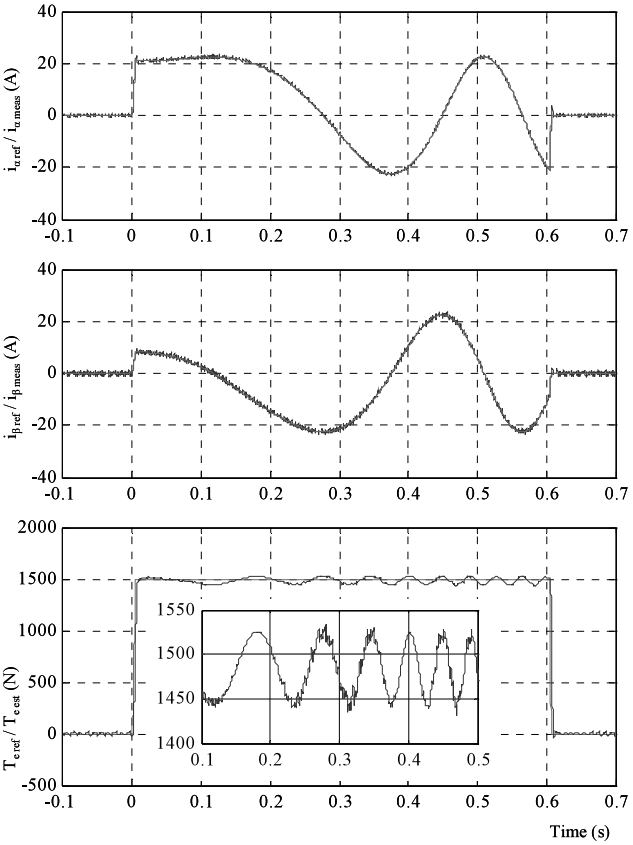

Fig. 8. AC current control system using one-frequency resonant controllers

5. Conclusion

In this paper, we have first analysed the influence of non-sinusoidal back-EMF on the thrust generated by this PMLSM. Based on the proposed optimal excitation current waveforms, a thrust control scheme has been established in the Concordia reference frame. The multiple-frequency resonant controllers have been used to regulate the load currents,

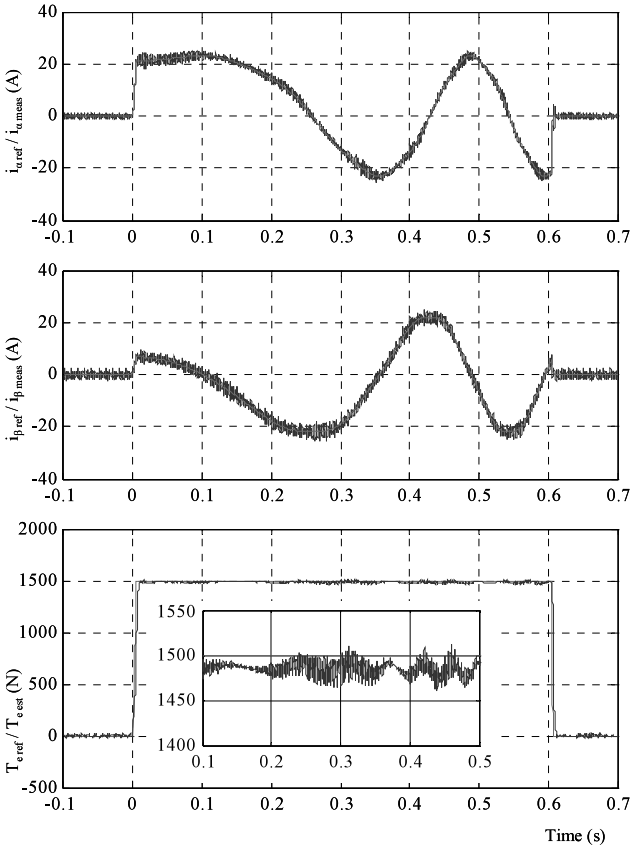

Fig. 9. AC current control system using teo-frequency resonant controllers

and morever, they compensate for the negative influence of back-EMF harmonics. Thanks to this type of controller, the load currents can perfectly track their respective references, and the thrust ripple caused by the back-EMF harmonics can be significantly reduced. The experimental results obtained from a laboratory test system verify the effectiveness of the suggested approach.

The next paper will be focused on the implementation issue of resonant controllers inside industrial CNC. Especially to respect short sample period (usually below 25 μs) required to achieve good control performances [23].

(Manuscript received Jan. 16, 2006,
revised July 7, 2006)

References

(1) A. Cassat, N. Corsi, N. Wavre, and R. Moser: "Direct Linear Drives: Market and Performance Status", LDIA2003, Birmingham, UK (2003-9)

(2) J.F. Gieras and Z.J. Piech: Linear Synchronous Motors: Transportation and Automation Systems, CRC Press (2000)

(3) P.J. Barre, A. Tounzi, J.P. Hautier, and S. Bouarouj: "Modelling and thrust control using resonnating controller of assymetrical PMLSM", EPE 2001, Graz, Austria, CD-ROM (2001)

(4) P.L. Chapman, S.D. Sudhoff, and C.A. Whitcomb: "Optimal Control Strategies for Surface-Mounted Permanent-Magnet Synchronous Machine Drives", *IEEE Trans. Energy Conversion*, Vol.14, No.4, pp.1043–1050 (1999)

(5) J.Y. Hung and Z. Ding: "Minimization of Torque Ripple in Permanent-Magnet Motors: A Closed Form Solution", Proceedings of the 18th IEEE Industrial Electronics Conference, pp.459–463 (1992)

(6) N.R.N. Idris and A.H.M. Yatim: "Reduced torque ripple and constant torque switching frequency strategy for direct torque control of induction machine",

Fifteenth Annual IEEE Applied Power Electronics Conference and Exposition, APEC 2000, Vol.1, pp.154–161 (2000-2)
(7) J. Faiz and B. Rezaei-Alam: "Control of a linear Permanent Magnet Synchronous Motor using Multiple Reference Frame Theory", Maglev 2002, Lausanne, Switzerland, pp.97–101 (2002-9)
(8) J.-K. Kang and S.-K. Sul: "New direct torque control of induction motor for minimum torque ripple and constant switching frequency", *IEEE Trans. Ind. Appl.*, Vol.35, No.5, pp.1076–1082 (1999-9/10)
(9) P.L. Chapman and S.D. Sudhoff: "A multiple reference frame synchronous estimator/regulator", *IEEE Trans. Energy Conversion*, Vol.15, No.2, pp.197–202 (2000-6)
(10) J.K. Kang and S.K. Sul: "Torque ripple minimization strategy for direct torque control of induction motor", in Conf. Rec. IEEE-IAS, pp.438–443 (1998)
(11) B.J. Kang and C.M. Liaw: "A robust hysteresis current-controlled PWM inverter for linear PMSM driven magnetic suspended positioning system", *IEEE Trans. Ind. Electron.*, Vol.48, No.5, pp.956–967 (2001-10)
(12) T.M. Jahns and W.L. Soong: "Pulsating Torque Minimization Techniques for Permanent Magnet AC Motor Drives—A Review", *IEEE Trans. Ind. Electron.*, Vol.43, No.2, pp.321–330 (1996)
(13) J. Zeng, X. Guillaud, and Ph. Degobert: "Control of AC machines with Multi-Frequency Resonant Controller", the 11th International Power Electronics and Motion Control Conference, EPE-PEMC2004, Riga, Latvia (2004-9)
(14) J. Zeng, P.J. Barre, and P. Degobert: "Modeling and Thrust Control of PMLSM using Principle of Local Energy", ICEMS2003, Beijing, P.R. China (2003)
(15) J. Zeng, G. Remy, P.J. Barre, and P. Degobert: "Analysis of the influence of the initial pole position on the PMLSM thrust performances—Application to high speed machine tool", LDIA2003, UK (2003-9)
(16) P.C. Krause, O. Wasynczuk, and S.D. Sudhoff: Analysis of Electrical Machinery, IEEE Press (1995)
(17) G. Remy, A. Tounzi, P.-J. Barre, F. Francis, and J.-P. Hautier: "Finite-Element Analysis of Non-Sinusoidal Electromotive Force in a Permanent Magnet Linear Synchronous Motor", The Fifth International Symposium on Linear Drives for Industry Applications, LDIA2005, kobe-Awaji, Japan (2005-9)
(18) J. Zeng, Ph. Degobert, D. Loriol, and JP. Hautier: "Robust Design of the Self-tuning Resonant Controller for AC current control systems", IEEE International Conference on Industrial Technology, ICIT 2005, Hong Kong (2005-12)
(19) S. Yaacob and F.A. Mohamed: "Real time self tuning controller for induction motor based on pole assignment method", Proceedings of the 37th International SICE Annual Conference. SICE'98 (1998-7)
(20) G. Lee, D. Jordan, and M. Sohrwardy: "A pole assignment algorithm for multivariable control systems", *IEEE Trans. Autom. Control*, Vol.24, No.2, pp.357–362 (1979-4)
(21) T.T. Lee and S.H. Lee: "Discrete optimal control with eigenvalue assigned inside a circular region", *IEEE Trans. Autom. Control*, Vol.31, No.10, pp.958–962 (1986-10)
(22) K. Furuta and S. Kim: "Pole assignment in a specified disk", *IEEE Trans. Autom. Control*, Vol.32, No.5, pp.423–427 (1987-5)
(23) P. Tiitinen: "The next motor control method, DTC direct torque control", in Proc. Int. Conf. Power Electronics, Drives and Energy System for Industrial Growth, Delhi, India, pp.37–43 (1996)

Remy Ghislain (Non-member) was born in France, in 1977. He received the teacher degree "agrégation" in 2001. He is presently a graduate teacher assistant and a PhD student in electrical engineering at l'Ecole Nationale Supérieure d'Arts et Métiers de Lille (ENSAM). His current research interests include modelling and control of linear synchronous motors.

Degobert Philippe (Non-member) was born in France, in 1963. He received a B.E. degree from the National Superior Academy of Arts and Trades (CNAM) in 1991; a PhD from the University of Science and Technology of Lille (USTL), France, in 1997. He has worked in an industrial R&D laboratory from 1984 to 1992, and he joined the Laboratory of Electrical Engineering and Power Electronics of Lille in 1992 (L2EP). He is currently an assistant professor at the Ecole Nationale Supérieure d'Arts et Métier de Lille (ENSAM). His main topics of interest concern the modeling and digital control of electrical machines. In the last few years, he has been interested in the integration of dispersed generation systems in electrical micro-grids.

Barre Pierre-Jean (Non-member) was born in France in 1957. He received the teacher degree "agrégation" in mechanical engineering in 1991 and the PhD in automatic in 1995 at the Ecole Nationale Supérieure d'Arts et Métier de Lille (ENSAM). He is currently Director and an assistant Professor at the ENSAM of Lille and Manager of a Technological Research Team in the field of control of high-dynamic machine-tools (ERTint. 1022 CEMODYNE). His current research interests include automatics, robotics and motion control.

Hautier Jean-Paul (Non-member) was born in France in 1948. He received the teaching degree "agrégation" in 1978 and the PhD in electrical engineering in 1984 at the University of Sciences and Technologies of Lille (France). He has been Professor since 1990 and Scientific Director since 2001 of the Ecole Nationale Supérieure d'Arts et Métier. Since 1991, he has been Director of Electrical Engineering Laboratory of Lille (L2EP). His current research interests include modelling, control and design of electrical and electromechanical systems.

Zeng Jia (Non-member) was born in China in 1976. In 1999, he received a B.E. degree in Industrial Automation from Tongji University, Shanghai, China; M.E. degree in Industrial Engineering from the ENSAM, Paris & Lille, France, in 2002; and the PhD degree in electrical engineering from the University of Sciences and Technologies of Lille (USTL), France, in 2005. Since then, he has been an Electronics Design Engineer with Schneider Electric. His research interests are electronics circuit design, motor control, and motion control systems.